Zitterbewegung and quantum revivals in monolayer graphene quantum dots in magnetic fields

Trinidad García,[1] Nicolás A. Cordero,[2] and Elvira Romera[3]

[1]*Department of Electronics and Computer Technology, Universidad de Granada, Fuentenueva s/n, 18071 Granada, Spain*
[2]*Physics Department, University of Burgos, Burgos, Spain*
[3]*Departamento de Física Atómica, Molecular y Nuclear and Instituto Carlos I de Física Teórica y Computacional,
Universidad de Granada, Fuentenueva s/n, 18071 Granada, Spain*

The wave-packet evolution in graphene quantum dots in magnetic fields has been theoretically studied. By analyzing an effective Hamiltonian model we show the wave-packet dynamics exhibits three types of periodicities (Zitterbewegung, classical, and revival times). The influence of the size of the quantum dot and the strength of the external magnetic field in these periodicities has been considered. In addition, we have found that valley degeneracy breaking is shown by both classical and revival times.

I. INTRODUCTION

In recent years there has been a growing interest in the study of the phenomenon introduced by Schrödinger in 1930 known as Zitterbewegung (ZB) [1]. This phenomenon appears in a Dirac particle as a rapid trembling motion around its rectilinear average trajectory, and it is a consequence of the interference between negative and positive energy eigenvalues. ZB has been studied theoretically, but has yet to be experimentally observed because its large oscillatory frequency and its small amplitude are not accessible experimentally at present [2]. Gerritsma *et al.* [3] have simulated experimentally the electron ZB by adjusting some parameters of the Dirac equation using trapped ions and lasers. In 2005 Zawadski [4] studied ZB in a semiconductor and Schliemann *et al.* [5] have studied the ZB in a semiconductor quantum well (QW). After these studies great interest emerged in the study of ZB in semiconductors (see Ref. [2] and references therein). Birwas and Ghosh [6] considered ZB of electrons in semiconductor QWs and quantum dots (QDs) in an in-plane magnetic field. Additionally, ZB has also been analyzed in detail in monolayer and bilayer graphene and in carbon nanotubes in recent years [2,7–14].

On the other hand, the quantum evolution of wave packets shows interesting revival phenomena. They have been studied over the past decades theoretically [15–17] and observed experimentally [18] in, for example, atoms, molecules, or Bose-Einstein condensates. Additionally, quantum revivals have been studied theoretically in low-dimensional quantum structures such as graphene, graphene quantum dots, and graphene quantum rings in perpendicular magnetic fields [2,12,13,19–25]. Revivals appear when a wave packet returns to a shape that is approximately the same as the initial one in the temporal evolution, and the time at which the revivals appear is called the revival time ($T_{\rm Re}$). This type of periodicity depends on the energy eigenvalue spectrum. Assuming an initial wave packet as a superposition of eigenstates sharply peaked around some level n_0, this wave packet initially will evolve with a semiclassical periodicity $T_{\rm Cl}$, and then it will spread and delocalize (collapse). At later times (integer multiples of the time $T_{\rm Re}/2$) it will recover its initial shape, oscillating semiclassically.

In this paper we will analyze the quantum revival and ZB phenomena in a monolayer graphene quantum dot in terms of

the size of the dot and by considering an external perpendicular magnetic field.

II. ZITTERBEWEGUNG AND REVIVALS IN GRAPHENE QUANTUM DOTS

A. Effective Hamiltonian

Let us consider a monolayer graphene quantum dot in a uniform perpendicular magnetic field. The effective Hamiltonian of this system can be written as [26]

$$H = v_F(\vec{p} + e\vec{A})\vec{\sigma} + \tau V(r)\sigma_z, \qquad (1)$$

where $\tau = \pm 1$ corresponds to the inequivalent corners K and K' of the Brillouin zone (respectively), $\vec{p}$ is the momentum, $\vec{A} = B/2(-y,x,0) = B/2(-r\sin\phi, r\cos\phi, 0)$ is the vector potential in Cartesian and polar coordinates (respectively), $v_F \approx 10^6$ m/s is the Fermi velocity, $\vec{\sigma}$ the Pauli matrices vector, and where the potential $V(r)$ is defined as [26]

$$V(r) = \begin{cases} 0, & r < R, \\ \infty, & r \geqslant R. \end{cases} \qquad (2)$$

We can solve the Dirac equation $H\Phi(r,\phi) = E\Phi(r,\phi)$ analytically as in Ref. [26]. The wave function is given by

$$\Phi(r,\phi) = e^{im\phi} \begin{pmatrix} \chi_1(r) \\ e^{i\phi}\chi_2(r) \end{pmatrix}, \qquad (3)$$

due to the fact that we can construct simultaneously eigenspinors for H and $J_z \equiv l_z + \frac{1}{2}\sigma_z$ because $[H,J_z] = (m + 1/2)$, where m is the eigenvalue of the third component of the angular momentum l_z, with m the angular momentum label. Now, introducing the spinor into the Dirac equation $H\Phi(r,\phi) = E\Phi(r,\phi)$, the following set of uncoupled differential equations are straightforwardly obtained:

$$\dot{\chi}_1(r) - m\chi_1(r)/r - r\chi_1(r)/2l_B^2 - \epsilon_2\chi_2(r) = 0, \qquad (4)$$

$$\dot{\chi}_2(r) + (m+1)\chi_2(r)/r + r\chi_2(r)/2l_B^2 + \epsilon_1\chi_1(r) = 0. \qquad (5)$$

In Eqs. (4) and (5) we have introduced the magnetic length $l_B = 1/\sqrt{eB}$ (we use $\hbar = 1$ throughout the paper) and $\epsilon_i = \tau\tilde{V} + \tilde{E}$, where $\tilde{V}$ and $\tilde{E}$ correspond to $V/(-iv_F)$ and $E/(-iv_F)$, respectively. Using the procedure described in
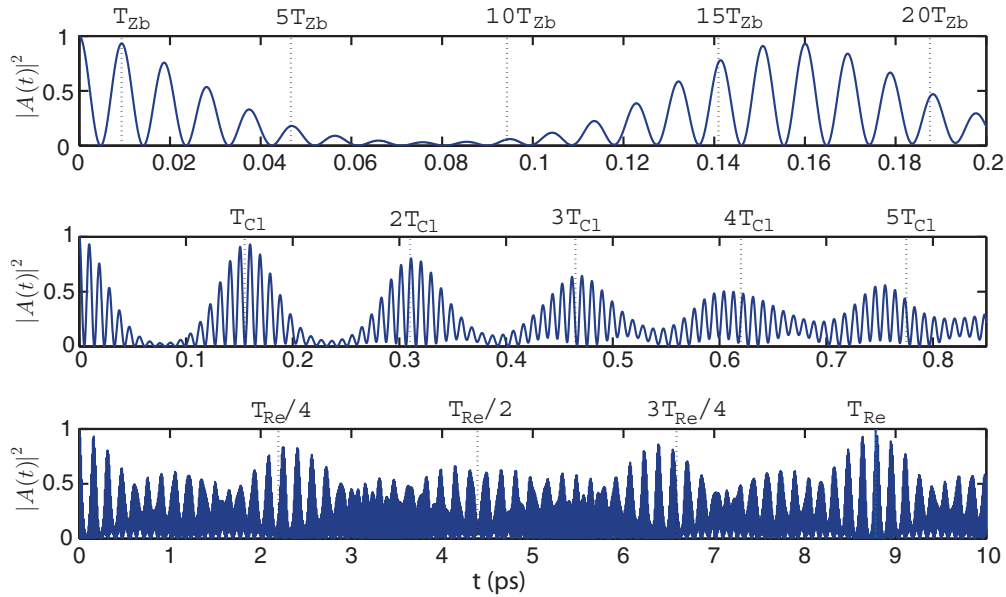
FIG. 1. (Color online) Time dependence of the autocorrelation function $|A(t)|^2$ in a graphene monolayer quantum dot for $B = 4$ T, $n_0 = 7$, $\sigma = 1$, and $R = 70$ nm in the K valley. ZB of the electrons with $T_{\rm Zb} \simeq 9.37$ fs (top). First classical periods of motion with $T_{\rm Cl} \simeq 0.157$ ps (middle). Long-time dependence with $T_{\rm Re} \simeq 8.74$ ps (bottom). The Zitterbewegung, classical, and main fractional revival periods are indicated by vertical dotted lines.

Ref. [26], the solutions are given by the confluent hypergeometric function of the second kind, $U(a,b,z)$, and the Laguerre polynomial $L(a,c,z)$. The eigenfunctions can be written as

$$\Phi_1(r,\phi) = c e^{im\phi} r^m e^{-r^2/4l_B^2}$$
$$\times L\left(k^2 l_B^2/2 - (m+1), m, r^2/2l_B^2\right), \quad (6)$$

$$\Phi_2(r,\phi) = c i e^{i(m+1)\phi} r^m e^{-r^2/4l_B^2} r/k l_B^2$$
$$\times \left[L\left(k^2 l_B^2/2 - (m+2), m+1, r^2/2l_B^2\right) \right.$$
$$\left. + L\left(k^2 l_B^2/2 - (m+1), m, r^2/2l_B^2\right) \right], \quad (7)$$

with the wave vector given by $E = v_F k$. Taking into account the boundary condition, the characteristic equation is obtained, and then the energy spectrum:

$$\left(1 - \tau \frac{k l_B^2}{R}\right) L\left(k^2 l_B^2/2 - (m+1), m, \frac{R^2}{2l_B^2}\right)$$
$$+ L\left(\frac{k^2 l_B^2 - 2(m+2)}{2}, m+1, \frac{R^2}{2l_B^2}\right) = 0. \quad (8)$$

B. Wave-packet revivals and ZB

The ZB of mobile charge carriers has been study in graphene during the past years (see the review in Ref. [2]). It has been studied in monolayer graphene, bilayer graphene, and carbon nanotubes.

Now, we will consider the wave-packet evolution in a monolayer graphene quantum dot in an external magnetic field. For this purpose we will construct an initial wave packet as a superposition of eigenstates of the Hamiltonian sharply concentrated around a large central value of the energy. As the initial localized wave packet is excited with an energy spectrum sharply peaked around n_0, we can consider the different time

scales from the coefficients of the Taylor expansion of the energy spectrum E_n around the energy E_{n_0}:

$$E_n \approx E_{n_0} + E'_{n_0}(n - n_0) + \frac{E''_{n_0}}{2}(n - n_0)^2 + \cdots. \quad (9)$$

The temporal evolution of the localized bound state Ψ for a time independent Hamiltonian can be written in terms of the eigenfunctions u_n and eigenvalues E_n as

$$\Psi = \sum_{n=0}^{\infty} a_n u_n e^{-i E_n t}, \quad (10)$$

with $a_n = \langle u_n, \Psi \rangle$, so taking into account (9),

$$e^{-i E_n t} = e^{-i(E_{n_0} + E'_{n_0}(n-n_0) + E''_{n_0}(n-n_0)^2/2 + \cdots)t}$$
$$= e^{-i\omega_0 t - 2\pi i(n-n_0)t/T_{\rm Cl} - 2\pi i(n-n_0)^2 t/T_{\rm Re} + \cdots}, \quad (11)$$

where each term in this exponential (except the first one which is a global phase) defines an important characteristic time scale, that is, $T_{\rm Re} \equiv \frac{4\pi}{|E''_{n_0}|}$ and $T_{\rm Cl} \equiv \frac{2\pi}{|E'_{n_0}|}$ (see Ref. [27] for more details). Besides analyzing revivals and quasiclassical periodicity, another important property, the ZB, has been studied. For this purpose we will take the Fermi energy as the energy origin and consider the population of both positive and negative energy levels. Let us denote the positive eigenvalues and the corresponding eigenfunctions as $E_n^{(+)}$ and $u_n^{(+)}$, respectively, and the negative ones as $E_n^{(-)}$ and $u_n^{(-)}$. Now let us consider an initial wave packet,

$$\psi = \frac{1}{\sqrt{2}}(\psi_+ + \psi_-) \quad \text{with } \psi_+ = \sum_{n=0}^{\infty} a_n u_n^{(+)},$$

$$\psi_- = \sum_{n=0}^{\infty} a_n u_n^{(-)}, \quad (12)$$
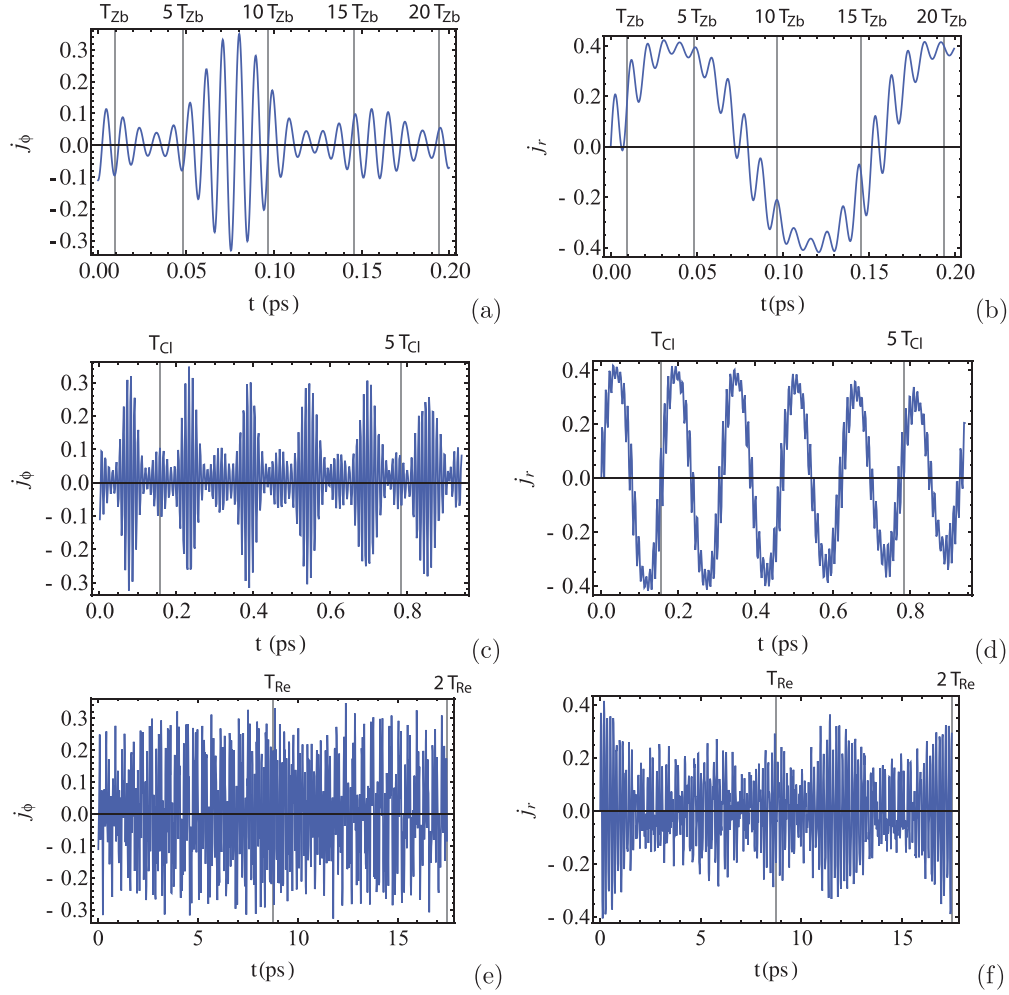
FIG. 2. (Color online) Time dependence of electric current j_ϕ and j_r (in pAm) in a graphene monolayer quantum dot for $B = 4$ T, $n_0 = 7$, $\sigma = 1$, and $R = 70$ nm in the K valley. (a), (b) ZB of the electrons with $T_{Zb} \simeq 9.37$ fs. (c), (d) First classical periods of motion with $T_{Cl} \simeq 0.157$ ps. (e), (f) Long-time dependence with $T_{Re} \simeq 8.74$ ps. The Zitterbewegung, classical, and main fractional revival periods are indicated by vertical dotted lines.

where the coefficients are Gaussianly distributed as

$$a_n = \frac{1}{\sqrt{\pi \sqrt{\sigma}}} e^{-(n-n_0)^2/2\sigma}, \tag{13}$$

and where we will take n_0 and n_0' such that

$$E_{n_0}^{(+)} \simeq -E_{n_0'}^{(-)}. \tag{14}$$

So, the time evolution of the wave packet is given by

$$\psi(t) = \sum_{n=0}^{\infty} a_n u_n^{(+)} e^{-iE_n^{(+)}t} + \sum_{n=0}^{\infty} a_n u_n^{(-)} e^{-iE_n^{(-)}t}. \tag{15}$$

In order to visualize the time evolution of the wave packets we will use the autocorrelation function

$$A(t) = \langle \Psi(t)|\Psi(0)\rangle, \tag{16}$$

that is, the overlap of the initial state $|\Psi(0)\rangle$ and its temporal evolution $|\Psi(t)\rangle$. Taking into account Eqs. (12) and (15), $A(t)$

is given by

$$A(t) = \sum_{n=0}^{\infty} |a_n|^2 e^{iE_n^{(+)}t} + \sum_{n=0}^{\infty} |a_n|^2 e^{iE_n^{(-)}t}. \tag{17}$$

By defining $E_{n_0} \equiv E_{n_0}^{(+)} \simeq -E_{n_0}^{(-)}$ and using Eq. (11), we obtain

$$A(t) = \sum_{n=0}^{\infty} |a_n|^2 e^{iE_{n_0}t + iE_{n_0}'(n-n_0)t + iE_{n_0}''(n-n_0)^2 t/2 + \cdots}$$

$$+ \sum_{n=0}^{\infty} |a_n|^2 e^{-iE_{n_0}t - iE_{n_0}'(n-n_0)t - iE_{n_0}''(n-n_0)^2 t/2 + \cdots}. \tag{18}$$

Since E_{n_0} is independent of n, $A(t)$ can be written up to order zero in the Taylor expansion as

$$A(t) = \sum_{n=0}^{\infty} |a_n|^2 e^{iE_{n_0}t + \cdots} + \sum_{n=0}^{\infty} |a_n|^2 e^{-iE_{n_0}t + \cdots}. \tag{19}$$

So, there is a global factor in $A(t)$ given by $2\cos(E_{n_0}t) = e^{-iE_{n_0}t} + e^{iE_{n_0}t}$ which defines another characteristic time

scale, the ZB time, given by $T_{Zb} \simeq \frac{2\pi}{|E_{n_0}|}$. So $A(t)$ exhibits the three characteristic periodicities, the ZB, the classical, and the revival times.

In the case of an infinite graphene monolayer in a magnetic field it has been shown that the ZB period, the classical period, and the revival time are given respectively by [13]

$$T_{Zb} = \frac{\pi}{\sqrt{2eB}v_F n_0^{1/2}}, \quad T_{Cl} = \frac{4\pi n_0^{1/2}}{\sqrt{2eB}v_F}, \quad T_{Re} = \frac{16\pi n_0^{3/2}}{\sqrt{2eB}v_F}, \quad (20)$$

where B is the strength of the magnetic field, v_F is the Fermi velocity, and e is the electron charge. Additionally, the time evolution of localized wave packets in graphene quantum dots in a perpendicular magnetic field has been studied [20], showing that the quasiclassical and revival periodicities appear for different values of the magnetic field intensities for a fixed value of the radius, and that the revival time is an observable sign of valley degeneracy breaking.

In this section, we will study the physical picture of wave-packet evolution in monolayer graphene quantum dots in an external magnetic field B for different values of the quantum dot radius R, focusing on the influence of this radius in quasiclassical and revival periodicities. We will also study ZB periodicity for different values of B and R in this system.

C. Numerical study

We have analyzed the time evolution of the wave packet as in Eq. (12) by using the autocorrelation function $A(t)$. We present in Fig. 1 the autocorrelation function for the time evolution in the K valley of a wave packet with $n_0 = 7$ and $\sigma = 1$ in a graphene monolayer quantum dot with $R = 70$ nm in a perpendicular magnetic field $B = 4$ T. As J_z commutes with H, we can choose a value m and we will take $m = 0$ for all the wave packets. Three different time scales are shown in the different panels. The top panel depicts the Zitterbewegung seen in the hundredth-of-a-picosecond scale, the middle panel shows the classical oscillation in the tenth-of-a-picosecond scale, while the revival of the wave function in the picosecond scale can be seen in the lower panel.

The middle panel displays how the regeneration of the wave packet is not perfect for each multiple of the classical time. It is necessary to wait for the revival time in order for the autocorrelation to recover a value close to unity, i.e., for a nearly perfect regeneration of the wave packet. This implies that, in particular, the Zitterbewegung amplitude regenerates at the revival time.

To investigate the behavior of electron currents we have calculated the r and ϕ components of them, given by

$$j_\phi = ev_F \langle \sigma_\phi \rangle, \quad j_r = ev_F \langle \sigma_r \rangle, \quad (21)$$

where $\sigma_\phi = \xi(\phi)\sigma_y$ and $\sigma_r = \xi(\phi)\sigma_x$, with

$$\xi(\phi) = \begin{pmatrix} e^{-i\phi} & 0 \\ 0 & e^{i\phi} \end{pmatrix}. \quad (22)$$

Figure 2 presents j_ϕ and j_r for the same initial wave packet and quantum dot as that in Fig. 1. It is clear from Figs. 2(a) and 2(b) that the electronic current is affected by ZB. At medium times there are quasiclassical oscillations [Figs. 2(c) and 2(d)].
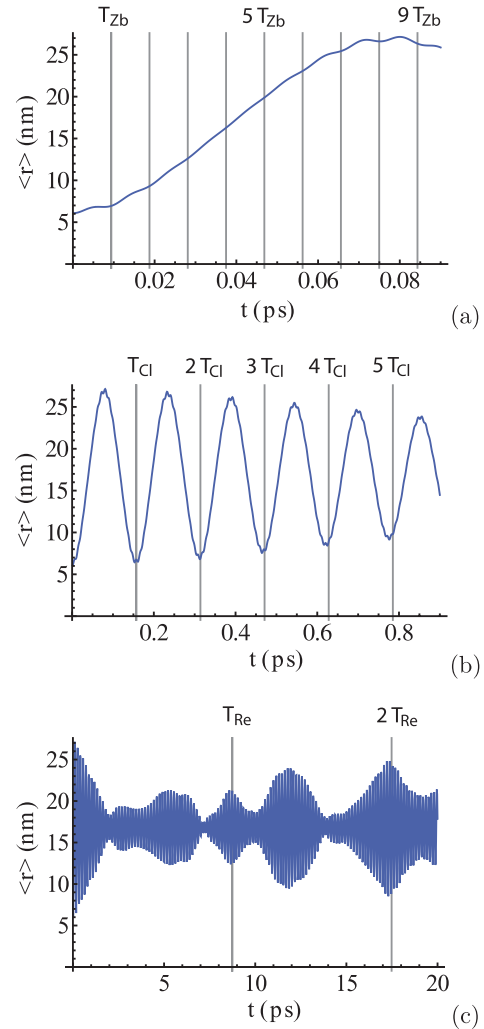
FIG. 3. (Color online) Time dependence of $\langle r \rangle$ in a graphene monolayer quantum dot for $B = 4$ T, $n_0 = 7$, $\sigma = 1$, and $R = 70$ nm in the K valley. (a) ZB of the electrons with $T_{Zb} \simeq 9.37$ fs. (b) First classical periods of motion with $T_{Cl} \simeq 0.157$ ps. (c) Long-time dependence with $T_{Re} \simeq 8.74$ ps. The Zitterbewegung, classical, and main fractional revival periods are indicated by vertical dotted lines.

Revivals can be identified clearly for j_r in Fig. 2(f), but they are not clear for j_ϕ in Fig. 2(e). We have also calculated the evolution of $\langle r \rangle$ and the results presented in Fig. 3 exhibit periodicities in the three time scales.

In order to study the effect of the magnetic field on the Zitterbewegung, classical, and revival times, we have calculated these three quantities for a graphene monolayer quantum dot with $R = 70$ nm in perpendicular magnetic fields ranging from 0 to 15 T. The results are presented in Fig. 4. The left panel in this figure shows that T_{Zb} is the same for K and K' valleys and decreases monotonically as B increases. The behavior is different for T_{Cl}, as can be seen in the central panel. First, the behavior is not monotonic. As the field grows, the semiclassical time first increases for low fields, then reaches a maximum, and finally decreases for strong fields. Second, for null or very intense perpendicular magnetic fields, there is no valley degeneracy breaking but the presence of moderate magnetic fields (0 T $< B \leqslant 11$ T) leads to higher classical
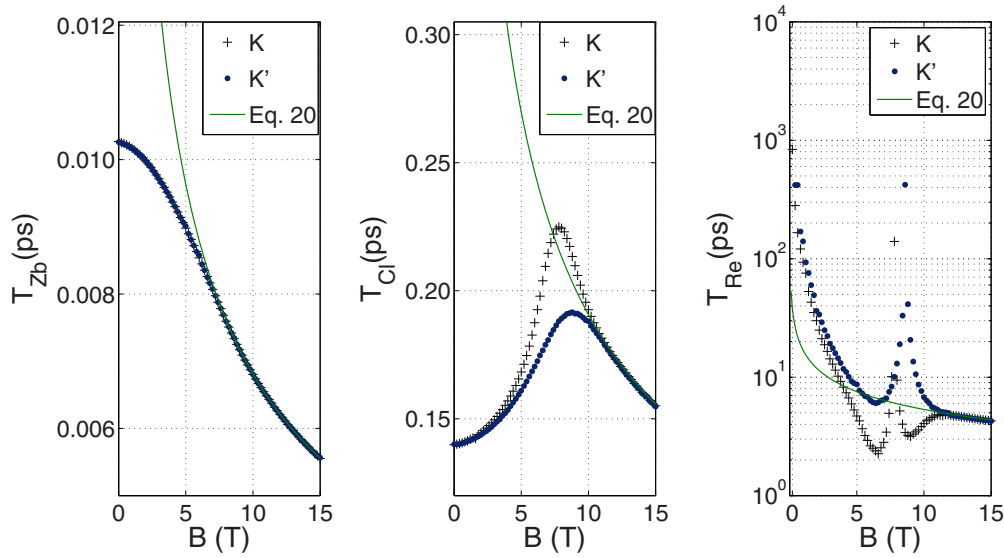
FIG. 4. (Color online) Wave-packet regeneration times for a graphene monolayer quantum dot with $R = 70$ nm in a perpendicular magnetic field as a function of the field intensity. The Zitterbewegung time is shown in the left panel, the classical time in the central panel, and the revival time in the right panel.

times in the K valley. The maximum for the K valley is located around 8 T while the maximum for the K' valley is around 9 T. Finally, the right panel shows the field dependence of the revival time. In this case there is first a decrease for low fields, then a sharp (note the logarithmic scale in the vertical axis) increase for intermediate fields, and finally a decrease for intense fields. Again, there is no valley degeneracy breaking for weak or strong fields, but this breaking appears for moderate fields (between 2 and 11 T). The maximum for the K valley is located around 8 T while the maximum for the K' valley is around 9 T.

We have also plotted the results for the three regeneration times obtained by using Eqs. (20), i.e., with the regeneration times for monolayer graphene (that can be seen as a quantum dot with an infinite radius). The agreement is excellent

for strong fields, poor for moderate fields, and disappears completely for weak fields. This means the behavior of these three times for a finite quantum dot is very different from that corresponding to an infinity graphene monolayer for weak fields, but tends to that of monolayer graphene as the field grows. This is a consequence of the dominant role played by the magnetic field in Eq. (1) that makes the size of the system not so important. This tendency is monotonic for the Zitterbewegung time but it is not so simple for the other two regeneration times. Interestingly, the minimum value of B for which Eqs. (20) are valid for a quantum dot with $R = 70$ nm is the same one at which the valley degeneracy breaking disappears.

We have also studied the effect of the magnetic field on the Zitterbewegung, classical, and revival times for a graphene
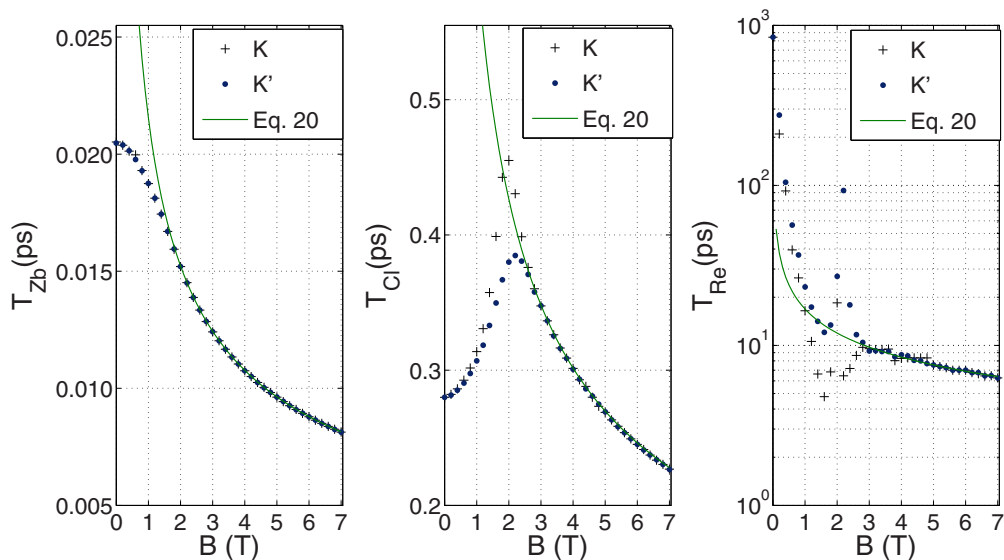
FIG. 5. (Color online) Same as Fig. 4 but for a graphene monolayer quantum dot with a radius $R = 140$ nm.
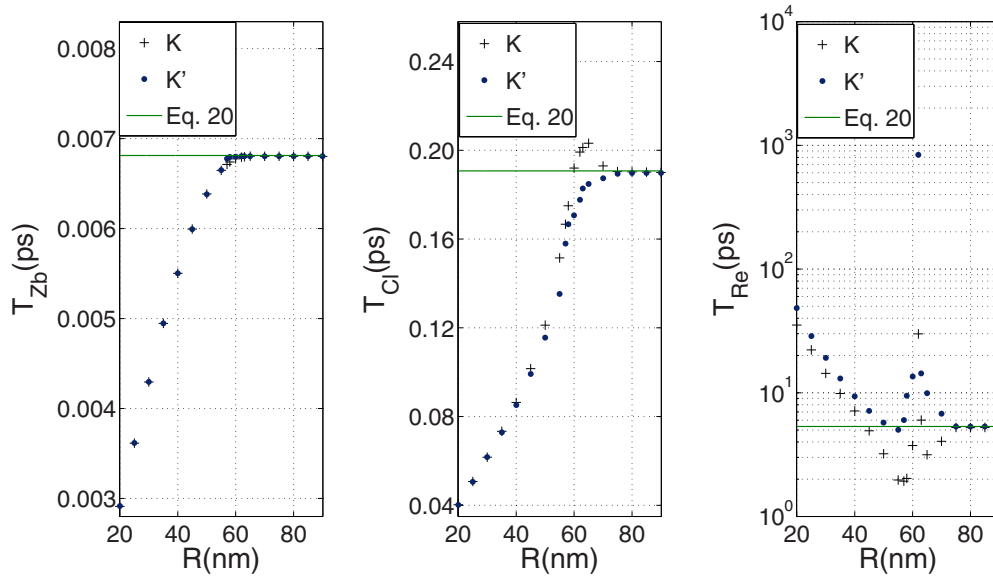
FIG. 6. (Color online) Wave-packet regeneration times for a graphene monolayer quantum dot in a perpendicular magnetic field $B = 10$ T as a function of the dot radius. The Zitterbewegung time is shown in the left panel, the classical time in the central panel, and the revival time in the right panel.

monolayer quantum dot with $R = 140$ nm in perpendicular magnetic fields ranging from 0 to 7 T. The results are presented in Fig. 5. They are qualitatively similar to those for the $R = 70$ nm case, but some quantitative differences arise. First, the peaks in both the classical and the revival times appear at lower fields (around 2 T for the K valley and around 2.2 T for the K' valley) and the separation between them decreases with respect to the $R = 70$ nm case. Second, the range of magnetic fields for which there is valley degeneracy breaking is smaller (0 T $< B \leqslant 3$ T). Third, the minimum value for which Eqs. (20) are valid for a quantum dot with $R = 140$ nm is lower than for $R = 70$ nm. This is easy to understand. The bigger the radius of the quantum dot, the better the approximation of considering the infinite radius case works. Nevertheless, once again, the minimum value of B for which Eqs. (20) are valid for a quantum dot with $R = 140$ nm is the same one at which the valley degeneracy breaking disappears.

We have performed similar calculations for other values of the radius and we have obtained analogous results. The dependence on the magnetic field is the following. The bigger the radius, (i) the narrower the peaks, the smaller their central values, and the smaller the separation between them, (ii) the smaller the range of magnetic fields for which there is valley degeneracy breaking, and (iii) as expected, the closer the results are to those of a graphene monolayer given by Eqs. (20).

In order to test if these general trends are valid for a wide range of dot sizes, we have calculated the three regeneration times for monolayer graphene quantum dots with several radii for different fixed perpendicular magnetic fields. As an example we present in Fig. 6 these times for quantum dots with radii between 20 and 90 nm in a perpendicular magnetic field $B = 10$ T. For small radii both Zitterbewegung and classical times grow with increasing radius while the revival time decreases. There is never valley degeneracy breaking for the Zitterbewegung time, but this breaking shows for both classical and revival times up to a certain radius (around 75 nm for the

$B = 10$ T case). This radius corresponds to the minimum size for the infinite radius approximation given by Eqs. (20) to become valid.

III. CONCLUSIONS

We have used an effective Hamiltonian in which a monolayer graphene quantum dot is described via an infinite cylindrical well. It is a simple model that allows to calculate analytically the wave function and that has been checked experimentally [26]. We have studied the regeneration of a wave packet built as a superposition of eigenstates sharply peaked around some energy level for a graphene monolayer quantum dot in a perpendicular magnetic field. Three different regeneration times (Zitterbewegung, classical, and revival) corresponding to three different time scales have been shown. We have analyzed quantum dots with different radii and in different magnetic fields. A common feature in this kind of system is that the revival time is always bigger than the classical time and the classical time is bigger than the Zitterbewegung time. Zitterbewegung time never shows valley degeneracy breaking while classical and revival times display this breaking for nonzero magnetic fields up to a radius that depends on the field but that always coincides with the minimum dot size for the infinite radius approximation (i.e., considering a graphene monolayer) to be valid. The behavior of both classical and revival times as a function of the field strength exhibits some common features: As the dot radius grows, the peaks get narrower, their central values become smaller and the peaks get closer, the valley degeneracy breaking magnetic field range gets smaller and, evidently, the times get closer to those for an infinite graphene monolayer sheet. We plan to make atomistic calculations using density functional theory methods [28] to test if all these conclusions hold with a more realistic model.

ACKNOWLEDGMENT

---

[1] E. Schrödinger, Sitzungsber. Preuss. Akad. Wiss. Phys.-Math. Kl. **24**, 418 (1930).

[2] See W. Zawadzki and T. M. Rusin, J. Phys.: Condens. Matter **23**, 143201 (2011) and references therein.

[3] R. Gerritsma, G. Kirchmair, F. Zahringer, E. Solano, R. Blatt, and C. F. Roos, Nature (London) **463**, 68 (2010).

[4] W. Zawadzki, Phys. Rev. B **72**, 085217 (2005).

[5] J. Schliemann, D. Loss, and R. M. Westervelt, Phys. Rev. Lett. **94**, 206801 (2005).

[6] T. Biswas and T. K. Ghosh, J. Phys.: Condens. Matter **24**, 185304 (2012).

[7] T. M. Rusin and W. Zawadzki, Phys. Rev. B **76**, 195439 (2007); **78**, 125419 (2008); **80**, 045416 (2009).

[8] E. McCann and V. I. Fal'ko, Phys. Rev. Lett. **96**, 086805 (2006).

[9] M. I. Katsnelson, Eur. Phys. J. B **51**, 157 (2006).

[10] G. M. Maksimova, V. Y. Demikhovskii, and E. V. Frolova, Phys. Rev. B **78**, 235321 (2008).

[11] J. C. Martinez, M. B. A. Jalil, and S. G. Tan, Appl. Phys. Lett. **97**, 062111 (2010)

[12] J. Schliemann, New J. Phys. **10**, 043024 (2008).

[13] E. Romera and F. de los Santos, Phys. Rev. B **80**, 165416 (2009).

[14] Y. X. Wang, Z. Yang, and S. J. Xiong, Eur. Phys. Lett. **89**, 17007 (2010)

[15] J. Parker and C. R. Stroud, Jr., Phys. Rev. Lett. **56**, 716 (1986).

[16] I. Sh. Averbukh and N. F. Perelman, Phys. Lett. A **139**, 449 (1989); Acta Phys. Pol., A **78**, 33 (1990).

[17] J. H. Eberly, N. B. Narozhny, and J. J. Sánchez-Mondragón, Phys. Rev. Lett. **44**, 1323 (1980).

[18] G. Rempe, H. Walther, and N. Klein, Phys. Rev. Lett. **58**, 353 (1987); J. A. Yeazell, M. Mallalieu, and C. R. Stroud Jr., *ibid.* **64**, 2007 (1990); M. J. J. Vrakking, D. M. Villeneuve, and A. Stolow, Phys. Rev. A **54**, R37 (1996); A. Rudenko *et al.*, Chem. Phys. **329**, 193 (2006); G. Della Valle, M. Savoini, M. Ornigotti, P. Laporta, V. Foglietti, M. Finazzi, L. Duò, and S. Longhi, Phys. Rev. Lett. **102**, 180402 (2009).

[19] V. Krueckl and T. Kramer, New J. Phys. **11**, 093010 (2009).

[20] J. J. Torres and E. Romera, Phys. Rev. B **82**, 155419 (2010).

[21] J. Luo, D. Valencia, and J. Lu, J. Chem. Phys. **135**, 224707 (2011).

[22] Y. Wang, Y. He, and S. Xiong, Mod. Phys. Lett. **26**, 1250139 (2012).

[23] A. López, Z. Z. Sun, and J. Schliemann, Phys. Rev. B **85**, 205428 (2012).

[24] V. Ya. Demikhovskii, G. M. Maksimova, A. A. Perov, and A. V. Telezhnikov, Phys. Rev. A **85**, 022105 (2012).

[25] T. Garcia, S. Rodriguez-Bolivar, N. A. Cordero, and E. Romera, J. Phys.: Condens. Matter **25**, 235301 (2013).

[26] S. Schnez, K. Ensslin, M. Sigrist, and T. Ihn, Phys. Rev. B **78**, 195427 (2008).

[27] R. W. Robinett, Phys. Rep. **392**, 119 (2004).

[28] I. G. Ayala, N. A. Cordero, and J. A. Alonso, Phys. Rev. B **84**, 165424 (2011).